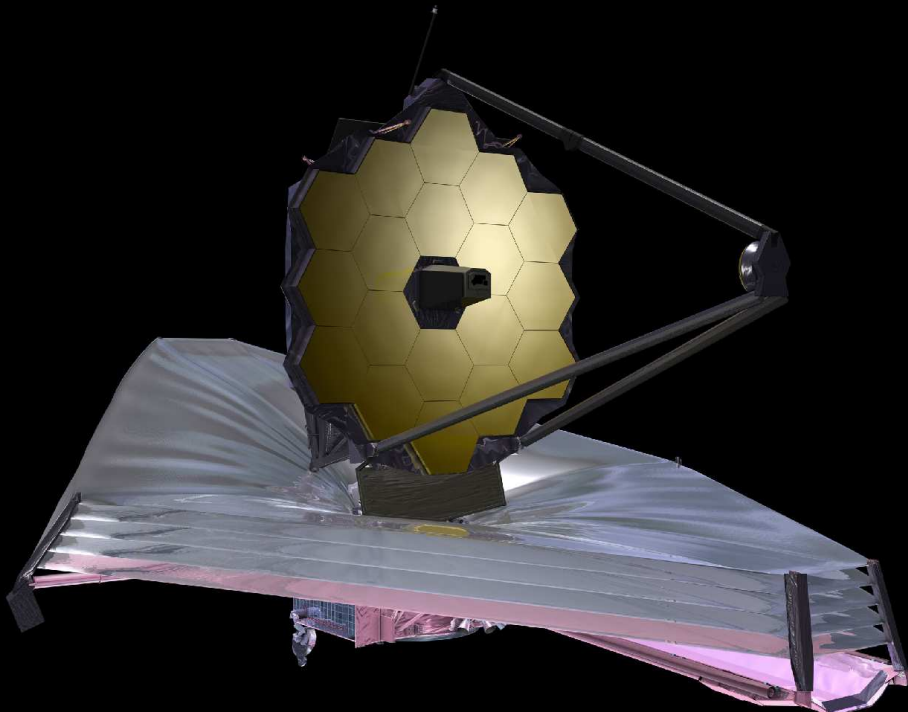


Astro 2020 Decadal Survey White Paper: Can JWST Detect Pop III Objects Directly via Caustic Transits?

Rogier Windhorst (ASU) — JWST Interdisciplinary Scientist

GTO team: T. Ashcraft, S. Cohen, R. Jansen, V. Jones, B. Joshi, D. Kim, B. Smith, F. Timmes, C. White (ASU), M. Alpaslan (NYU), D. Coe, N. Grogin, N. Hathi, A. Koekemoer, N. Pirzkal, A. Riess, R. Ryan, L. Strolger (STScI), C. Conselice, I. Smail (UK), W. Brisken, J. Condon, W. Cotton, K. Kellermann, R. Perley (NRAO), J. Diego, T. Broadhurst, (Spain), S. Driver, R. Livermore, M. Marshall, A. Robotham, S. Wyithe (OZ), K. Duncan, H. Rottgering (Leiden), S. Finkelstein, R. Larson (UT), G. Fazio, M. Ashby, P. Maksym (CfA), B. Frye, M. Rieke, C. Willmer (UofA), H. Hammel (AURA), G. Hasinger (ESA), A. Kashlinsky, S. Milam, A. Straughn (GSFC), W. Keel (U-AL), P. Kelly (U-MN), P. S. Rodney (U-SC), M. Rutkowski (MNSU), H. Yan (U-MO), A. Zitrin (Israel).



- Today, the JWST science remains as compelling as it was \sim 20 years ago.
- In fact, the JWST science is far more exciting today than we could have imagined or planned for \sim 20 years ago.

Talk at the JWST Science Working Group — Apr. 3, 2019

Talk is on: http://www.asu.edu/clas/hst/www/jwst/jwsttalks/jwst_caustictransitsWP_03apr19.pdf

Outline & Conclusions

- (1a) The principle of cluster caustic transits: Extreme magnifications.
- (1b) HST observations of OB-star caustic transits at $z \simeq 1-1.5$
- (2a) Limits to the SKY-SB of Pop III objects: First Stars
- (2b) Limits to the SKY-SB of Pop III objects: Black Holes
- (3) Conclusions:
 - In the best lensing clusters, JWST may detect caustic transits of Pop III stars and their stellar-mass black hole accretion disks at $z \gtrsim 7$.
 - It will need to monitor $\gtrsim 3$ clusters for years to see this.

(1a) The principle of cluster caustic transits: Extreme magnifications.

THE ASTROPHYSICAL JOURNAL SUPPLEMENT SERIES, 234:41 (40pp), 2018 February
© 2018. The American Astronomical Society. All rights reserved.

<https://doi.org/10.3847/1538-4365/aaa760>



On the Observability of Individual Population III Stars and Their Stellar-mass Black Hole Accretion Disks through Cluster Caustic Transits

Rogier A. Windhorst¹, F. X. Timmes¹, J. Stuart B. Wyithe², Mehmet Alpaslan³, Stephen K. Andrews⁴, Daniel Coe⁵, Jose M. Diego⁶, Mark Dijkstra⁷, Simon P. Driver⁴, Patrick L. Kelly⁸, and Duho Kim¹

¹ School of Earth and Space Exploration, Arizona State University, Tempe, AZ 85287-1404, USA; Rogier.Windhorst@asu.edu, Francis.Timmes@asu.edu

² University of Melbourne, Parkville, VIC 3010, Australia; SWyithe@physics.unimelb.edu.au

³ New York University, Department of Physics, 726 Broadway, Room 1005, New York, NY 10003, USA

⁴ The University of Western Australia, 35 Stirling Highway, Crawley, WA 6009, Australia

⁵ Space Telescope Science Institute, 3700 San Martin Drive, Baltimore, MD 21218, USA

⁶ IFCA, Instituto de Física de Cantabria (UC-CSIC), Avenida de Los Castros s/n, E-39005 Santander, Spain

⁷ Institute of Theoretical Astrophysics, University of Oslo, NO-0315 Oslo, Norway

⁸ University of California at Berkeley, Berkeley, CA 94720-3411, USA

Received 2017 November 22; revised 2018 January 6; accepted 2018 January 10; published 2018 February 14

Abstract

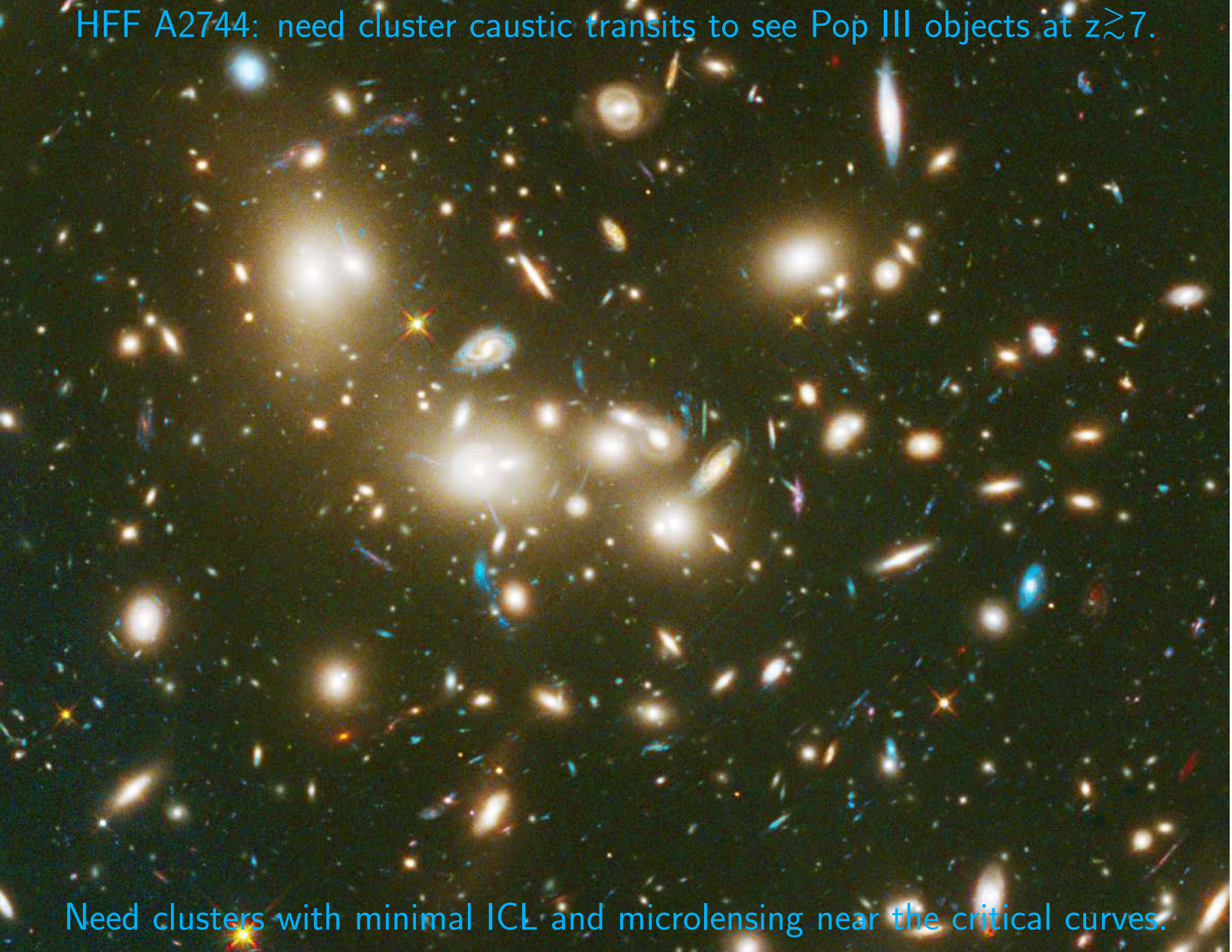
We summarize panchromatic Extragalactic Background Light data to place upper limits on the integrated near-infrared surface brightness (SB) that may come from Population III stars and possible accretion disks around their stellar-mass black holes (BHs) in the epoch of First Light, broadly taken from $z \simeq 7\text{--}17$. Theoretical predictions and recent near-infrared power spectra provide tighter constraints on their sky signal. We outline the physical properties of zero-metallicity Population III stars from MESA stellar evolution models through helium depletion and of BH accretion disks at $z \gtrsim 7$. We assume that second-generation non-zero-metallicity stars can form at higher multiplicity, so that BH accretion disks may be fed by Roche-lobe overflow from lower-mass companions. We use these near-infrared SB constraints to calculate the number of caustic transits behind lensing clusters that the *James Webb Space Telescope* and the next-generation ground-based telescopes may observe for both Population III stars and their BH accretion disks. Typical caustic magnifications can be $\mu \simeq 10^4\text{--}10^5$, with rise times of hours and decline times of $\lesssim 1$ year for cluster transverse velocities of $v_T \lesssim 1000 \text{ km s}^{-1}$. Microlensing by intracluster-medium objects can modify transit magnifications but lengthen visibility times. Depending on BH masses, accretion-disk radii, and feeding efficiencies, stellar-mass BH accretion-disk caustic transits could outnumber those from Population III stars. To observe Population III caustic transits directly may require monitoring 3–30 lensing clusters to AB $\lesssim 29$ mag over a decade.

Key words: accretion, accretion disks – galaxies: clusters: general – gravitational lensing: strong – infrared: diffuse background – stars: black holes – stars: Population III

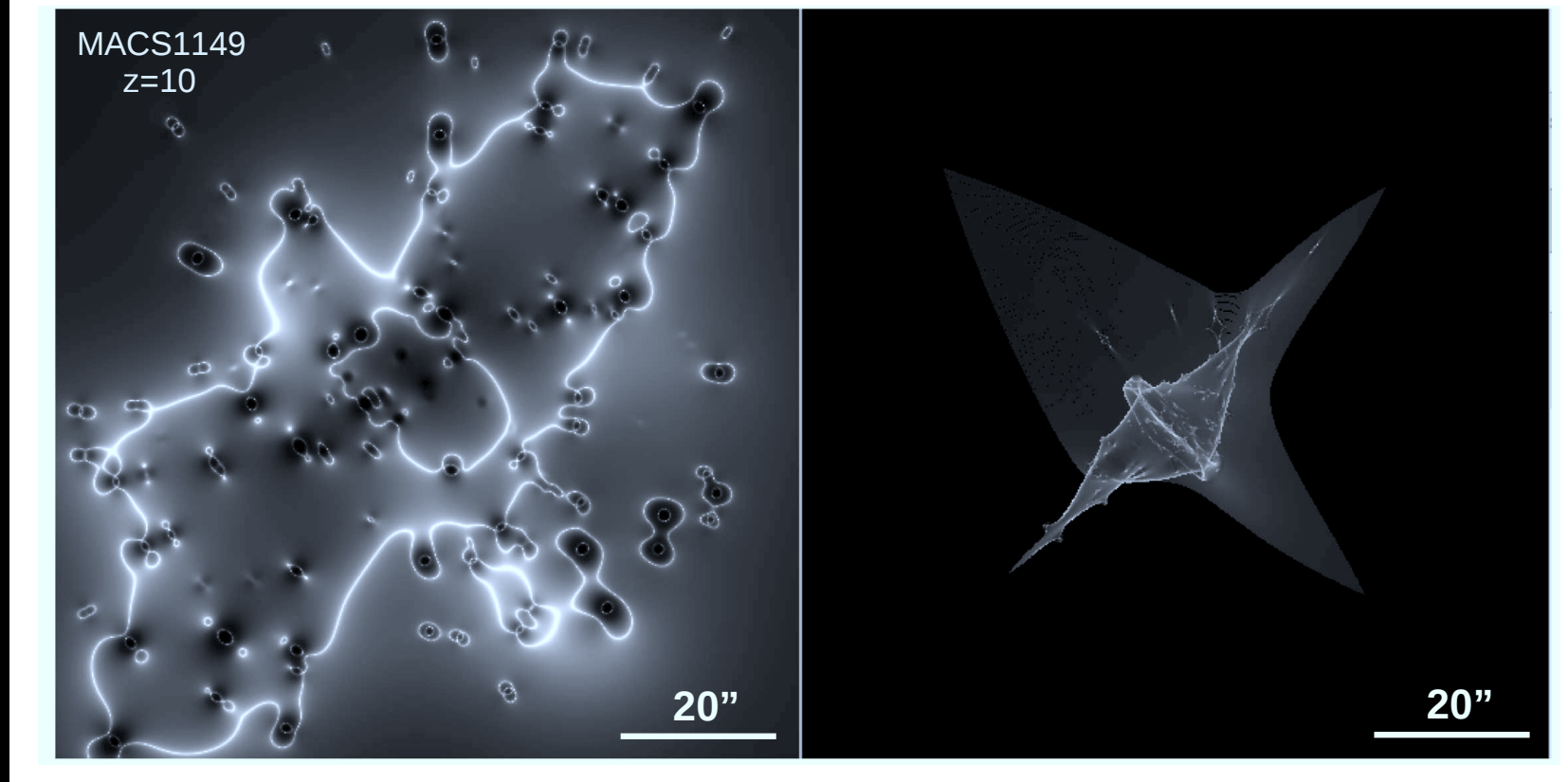
Windhorst⁺ (2018, ApJS, 234, 41): JWST (and 25–39 m ground-based telescopes?) may detect Pop III stars and their stellar-mass BH accretion disks *directly* to AB $\lesssim 28\text{--}29$ mag via caustic transits in the right clusters.

- JWST GO community should anticipate this and build on it.

HFF A2744: need cluster caustic transits to see Pop III objects at $z \gtrsim 7$.



Need clusters with minimal ICL and microlensing near the critical curves.



For source at $z=10$, critical curves for HFF cluster MACS 1149 at $z \simeq 0.54$ [LEFT], and main cluster caustics [in the source plane; RIGHT].

- Transverse cluster (sub-component) velocities can be $v_T \lesssim 1000$ km/s (Kelly⁺ 2018; Nature Astr. 2, 334; Windhorst⁺ 2018, ApJS, 234, 41).
- Main caustic magnification: $\mu \simeq 10 / (\text{d}_{\text{caustic}}/\text{"})^{1/2}$. For Pop III objects at $z \gtrsim 7$ with $1-30 R_\odot$, μ can then be $\gtrsim 10^4 - 10^5$ for $\lesssim 0.4$ year.
- Must use clusters with minimal ICL near the critical curves, since ICL microlensing dilutes the main caustics (Diego⁺ 2018, ApJ, 857, 25).

(1b) HST observations of OB-star caustic transits at $z \approx 1$ -1.5

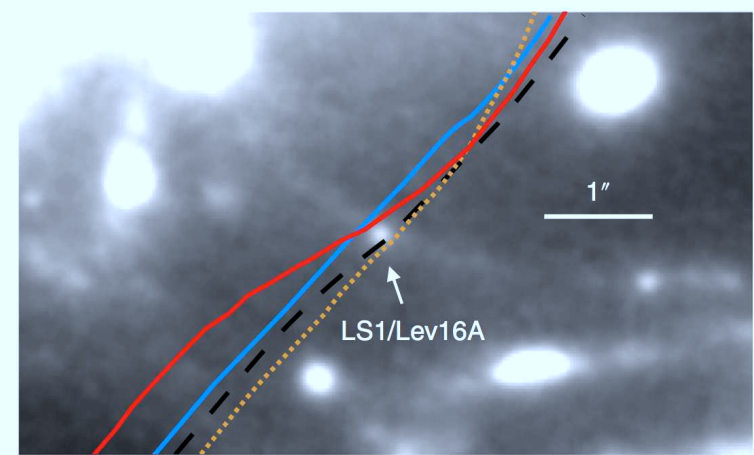
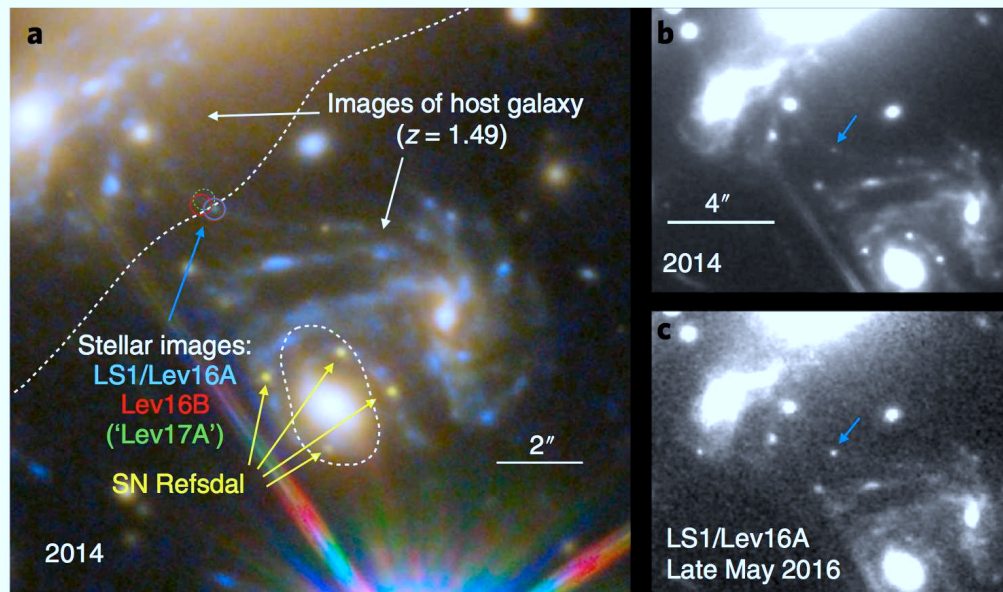


Fig. 2 | Proximity of LS1/Lev16A to the MACS J1149 galaxy cluster's critical curve for multiple galaxy-cluster lens models. Critical curves for models with available high-resolution lens maps including ref. ⁸ (CATS;

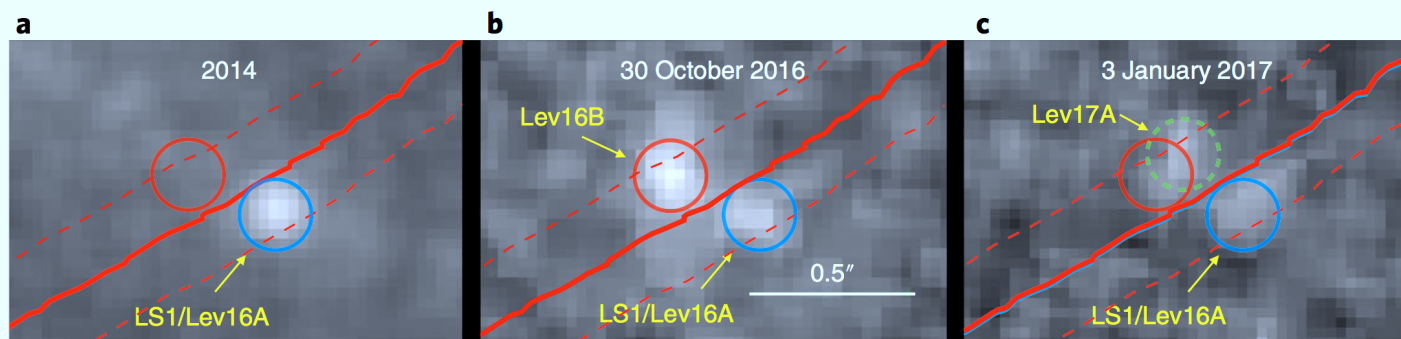


Fig. 5 | Highly magnified stellar images located near the MACS J1149 galaxy cluster's critical curve. **a**, LS1 in 2014; we detected LS1 when it temporarily brightened by a factor of ~4 in late April 2016, and its position is marked by a blue circle. **b**, The appearance of a new image dubbed Lev16B on 30 October 2016, whose position is marked by a red circle. The solid red line marks the location of the cluster's critical curve from the CATS cluster model⁸, and the dashed red lines show the approximate 1σ uncertainty from comparison of multiple cluster lens models⁵⁻¹⁰. Lev16B's position is consistent with the possibility that it is a counterimage of LS1. **c**, The candidate named Lev17A at the location of the green dashed circle had a $\sim 4\sigma$ significance detection on 3 January 2017. If a microlensing peak, Lev17A must correspond to a different star.

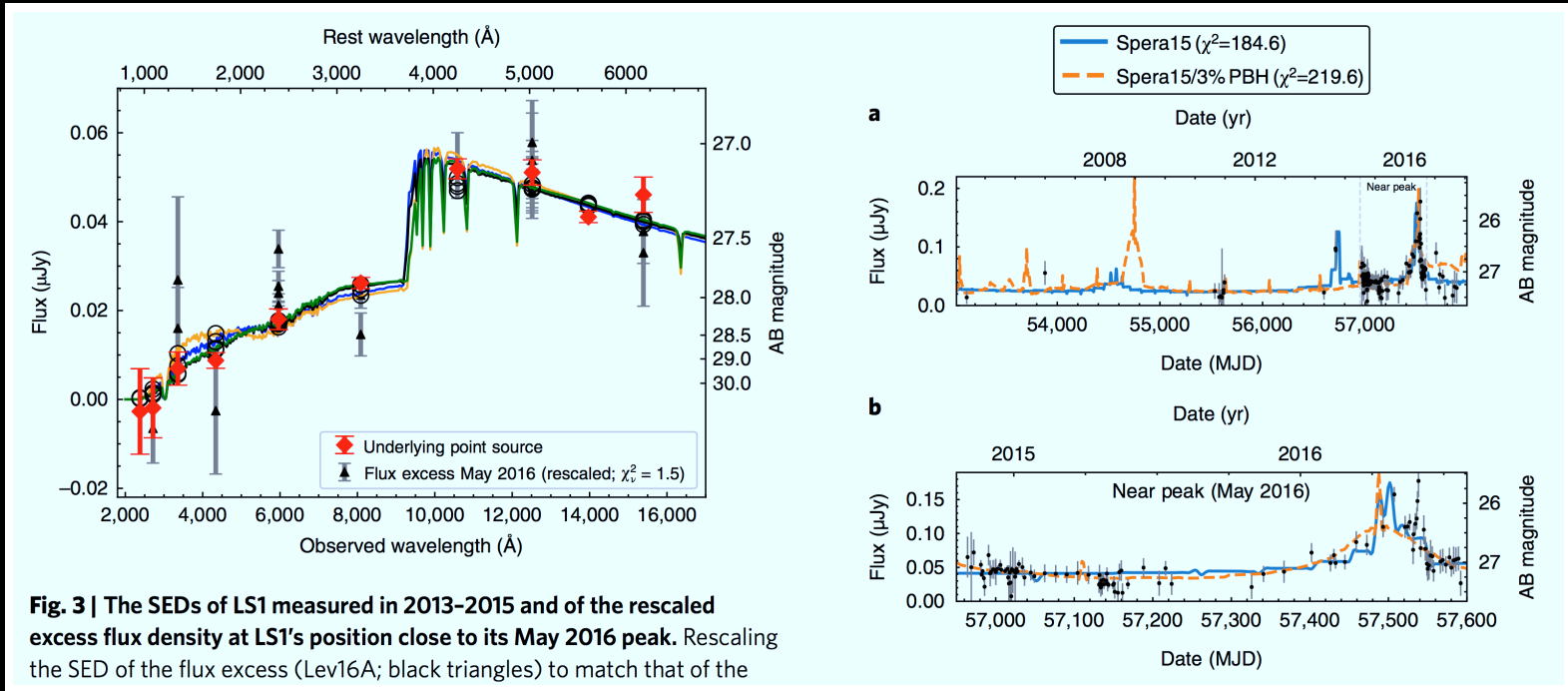


Fig. 3 | The SEDs of LS1 measured in 2013–2015 and of the rescaled excess flux density at LS1’s position close to its May 2016 peak. Rescaling the SED of the flux excess (Lev16A; black triangles) to match that of the

Kelley et al. 2018 (Nat. Astr. 2, 334): caustic transit of a B-star at $z \approx 1.49$.

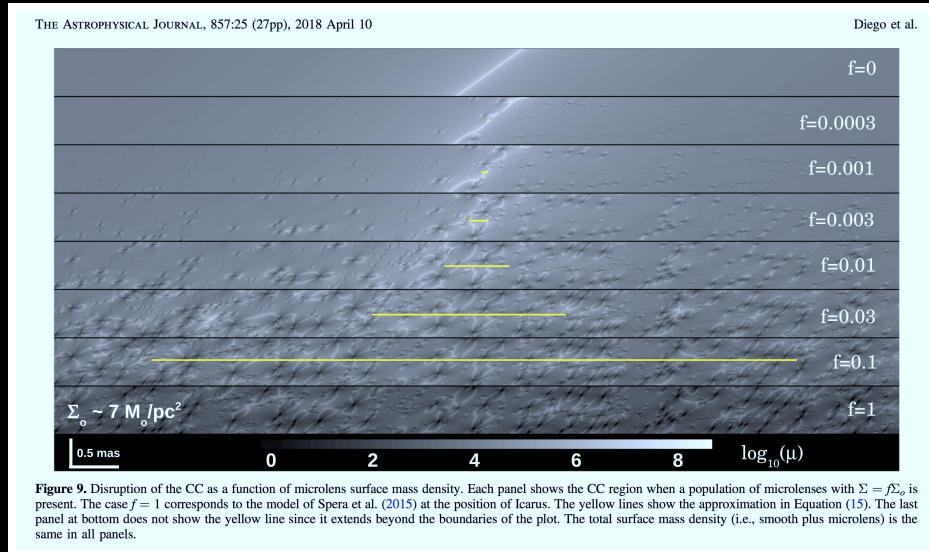
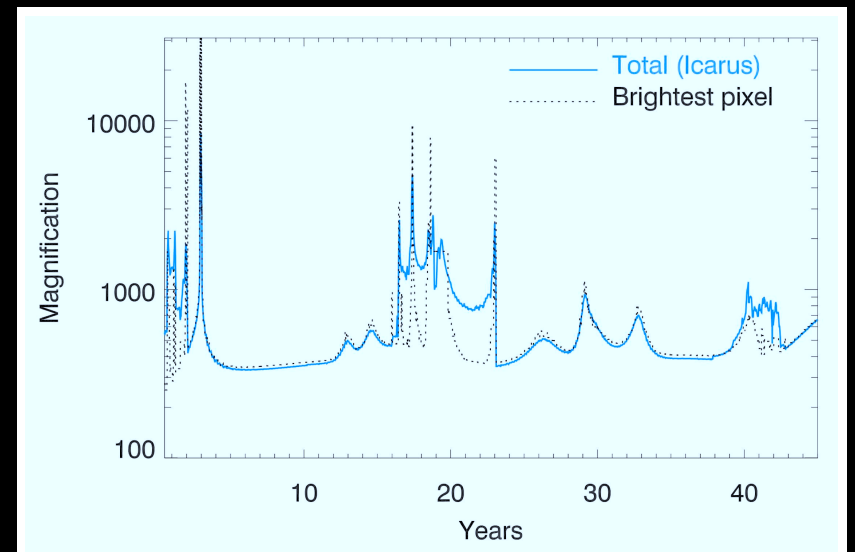
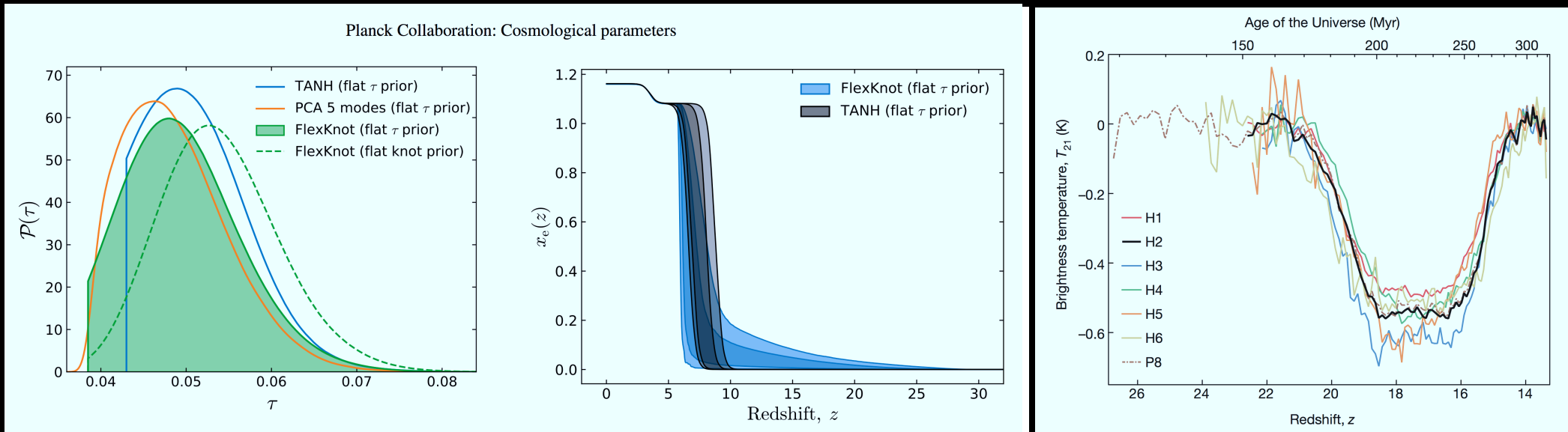


Figure 9. Disruption of the CC as a function of microlens surface mass density. Each panel shows the CC region when a population of microlenses with $\Sigma = f\Sigma_o$ is present. The case $f = 1$ corresponds to the model of Spera et al. (2015) at the position of Taurus. The yellow lines show the approximation in Equation (15). The last panel at bottom does not show the yellow line since it extends beyond the boundaries of the plot. The total surface mass density (i.e., smooth plus microlens) is the same in all panels.



Diego⁺ 2018 (ApJ, 857, 25): caustic transits in the presence of microlensing.
See also Miralda-Escudé (1991), Venumadhav et al. (2017, ApJ, 850, 49).

(2a) Limits to the SKY-SB of Pop III objects: First Stars

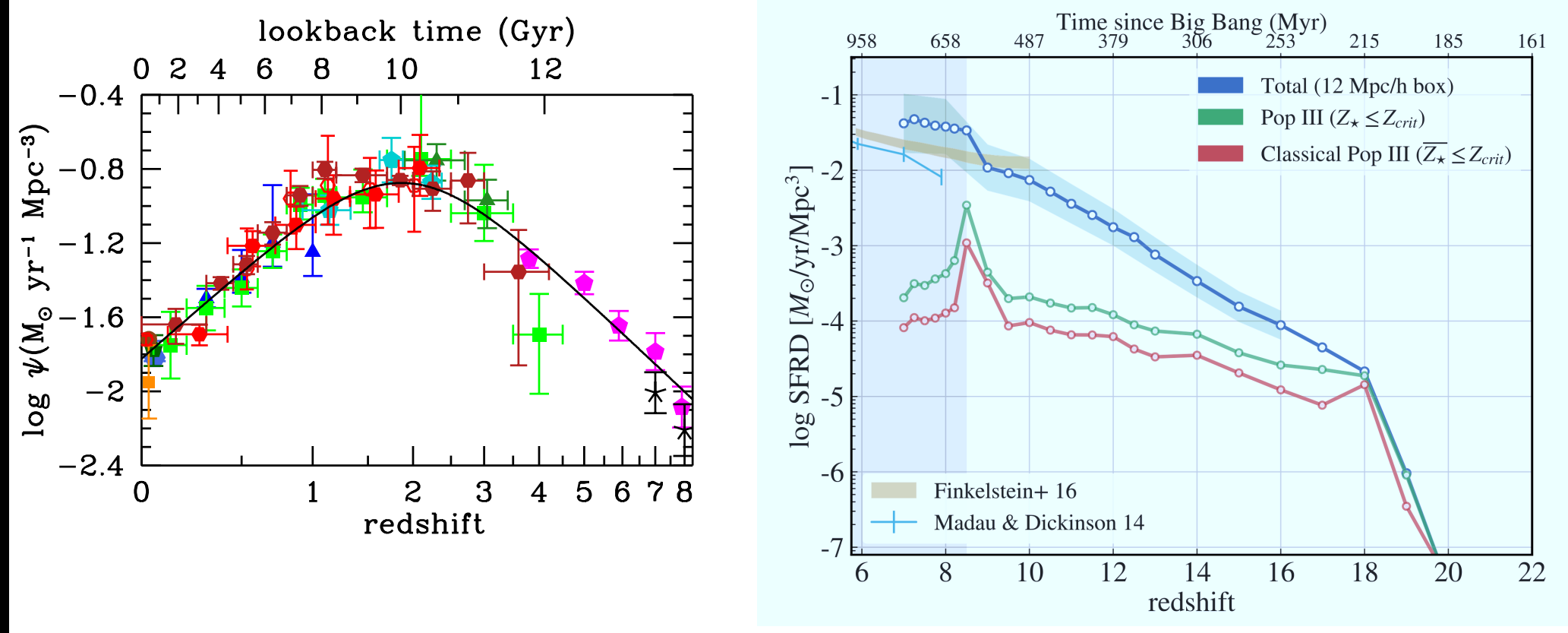


Two Reionization/First Light constraints remain seemingly at odds:

[LEFT 2]: Planck 2018 VI (astro-ph/1807.06209v1): ● Cosmic Background polarization $\tau \simeq 0.054 \pm 0.007 \Rightarrow z_{reion} \simeq 7.7 \pm 0.7$ (age 670 Myr).

[RIGHT]: Bowman et al. EDGES result (2018, Nature, 555, 67):

- Possible global 78 MHz HI-signal at $z \simeq 17 \pm 2$ (age 225 Myr).
- How can we reconcile this in context of the First Stars?
- What does this mean for First Dust, and the first (BH) binary stars?



Anticipated cosmic star-formation rate (SFR) at $z \gtrsim 7$:

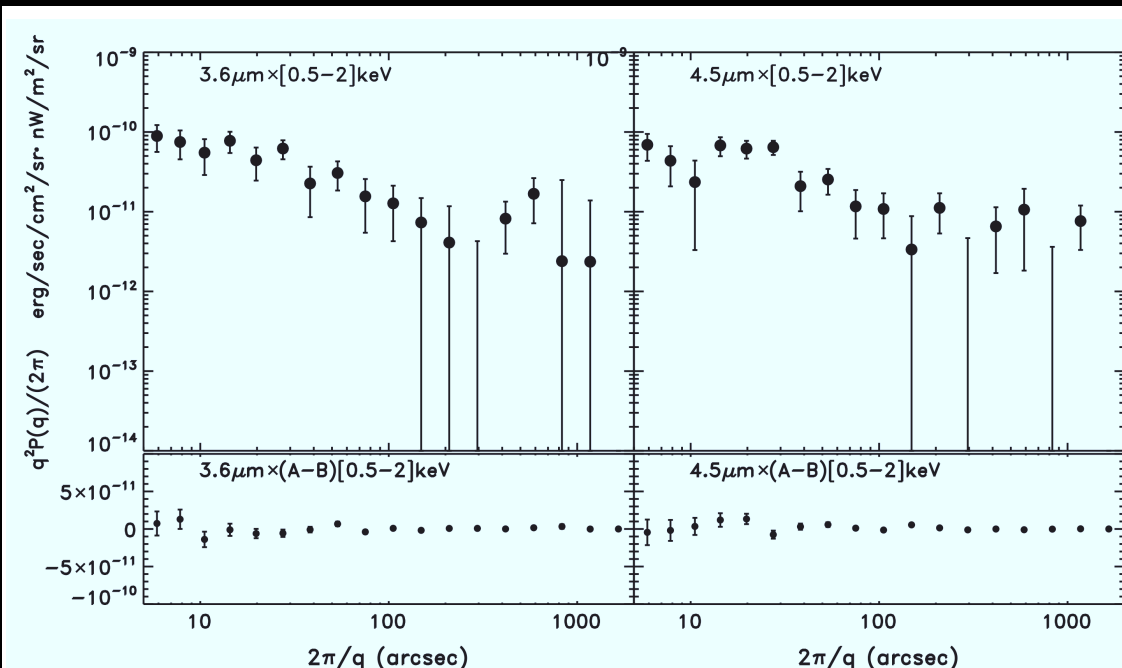
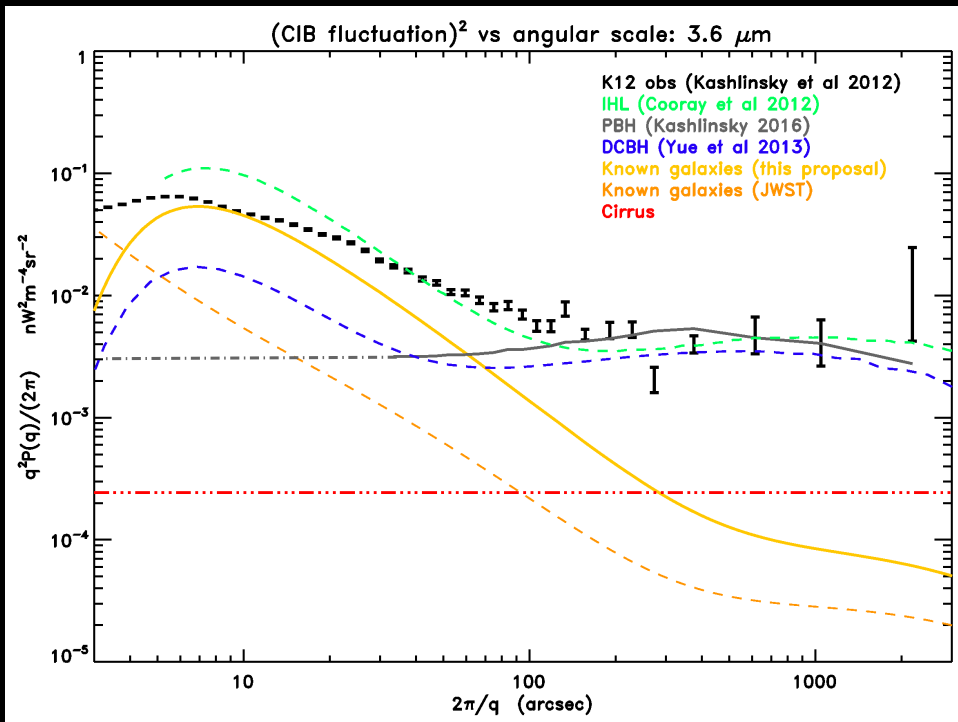
[LEFT] Observed (e.g., Madau & Dickinson; 2014, ARAA, 52, 415);

[RIGHT] RAMSES models (e.g., Sarmento et al. 2018, ApJ, 854 75).

⇒ Adopt this SFR from $z \simeq 17$ to $z \simeq 7$, implying at the lowest masses:

- Metallicity increases from ~ 0 at $z \simeq 18$ to $\lesssim 10^{-3}$ solar at $z \simeq 7$.
- ⇒ First Stars may go quickly from forming singly (at $z \simeq 17$) to forming in binaries (at $z \lesssim 7$) ⇒ Integrated sky-SB(SFR $z \gtrsim 7$) $\gtrsim 31$ mag/arcsec 2 .

(2b) Limits to the SKY-SB of Pop III objects: Stellar Mass Black Holes

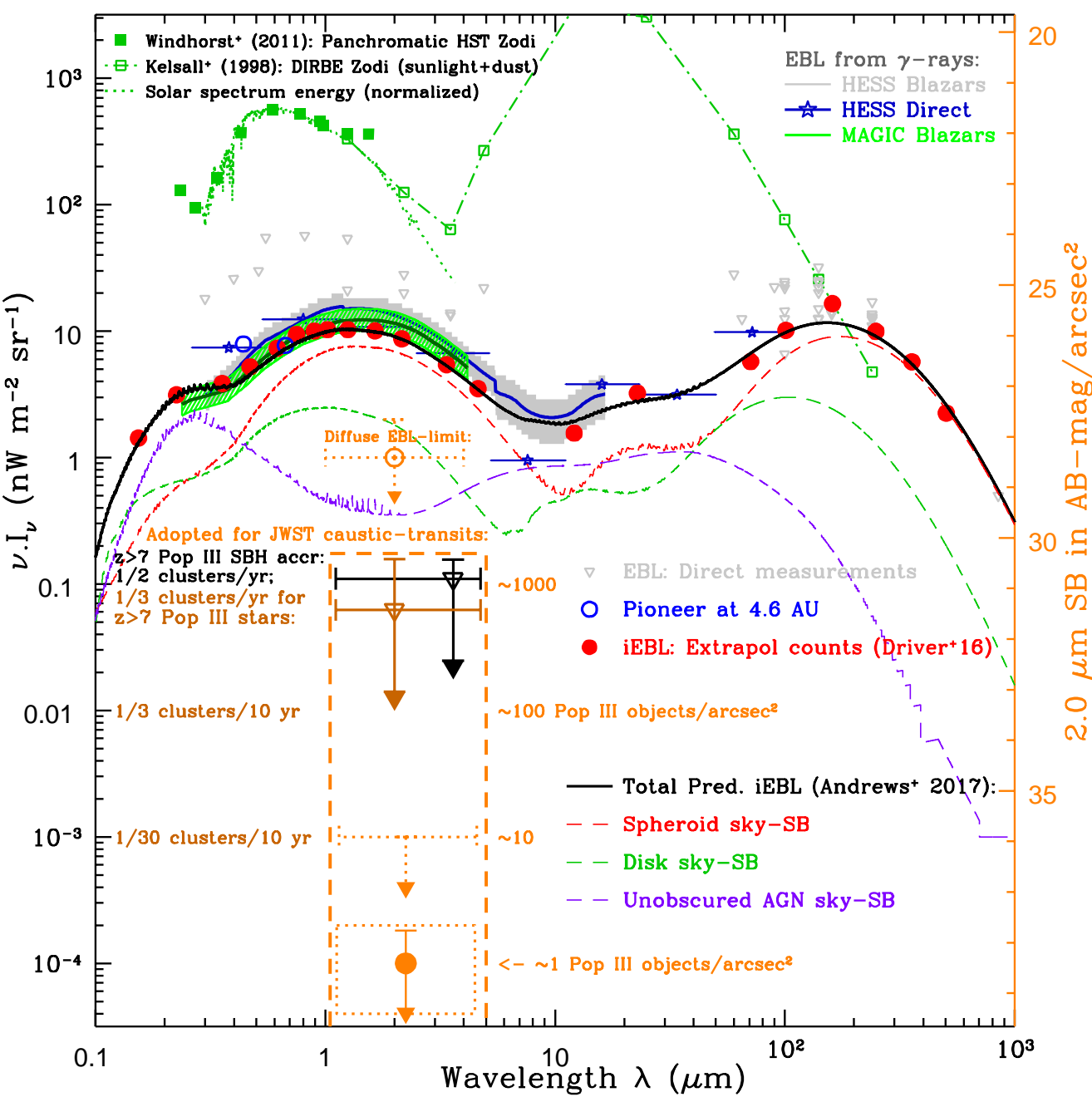


[LEFT] Object-free Spitzer $3.6\mu\text{m}$ power-spectrum constrains noise fluctuation models (Cappelluti et al. 2017; Kashlinsky et al. 2012, 2015, 2018):

Explainable by: Primordial black hole or Direct-collapse black hole models.

[RIGHT] Spitzer–Chandra cross-corr spectrum (Mitchell-Wynne et al. 2016):

- Objects at $z \gtrsim 7$ have sky-SB $\simeq 31$ mag/arc s^2 , plus likely a (stellar mass) black hole X-ray component. (Kashlinsky+ 2018; Windhorst+ 2018, ApJ, 234, 41).



Extragalactic Background Light (Driver⁺ 16; Windhorst⁺ 18):

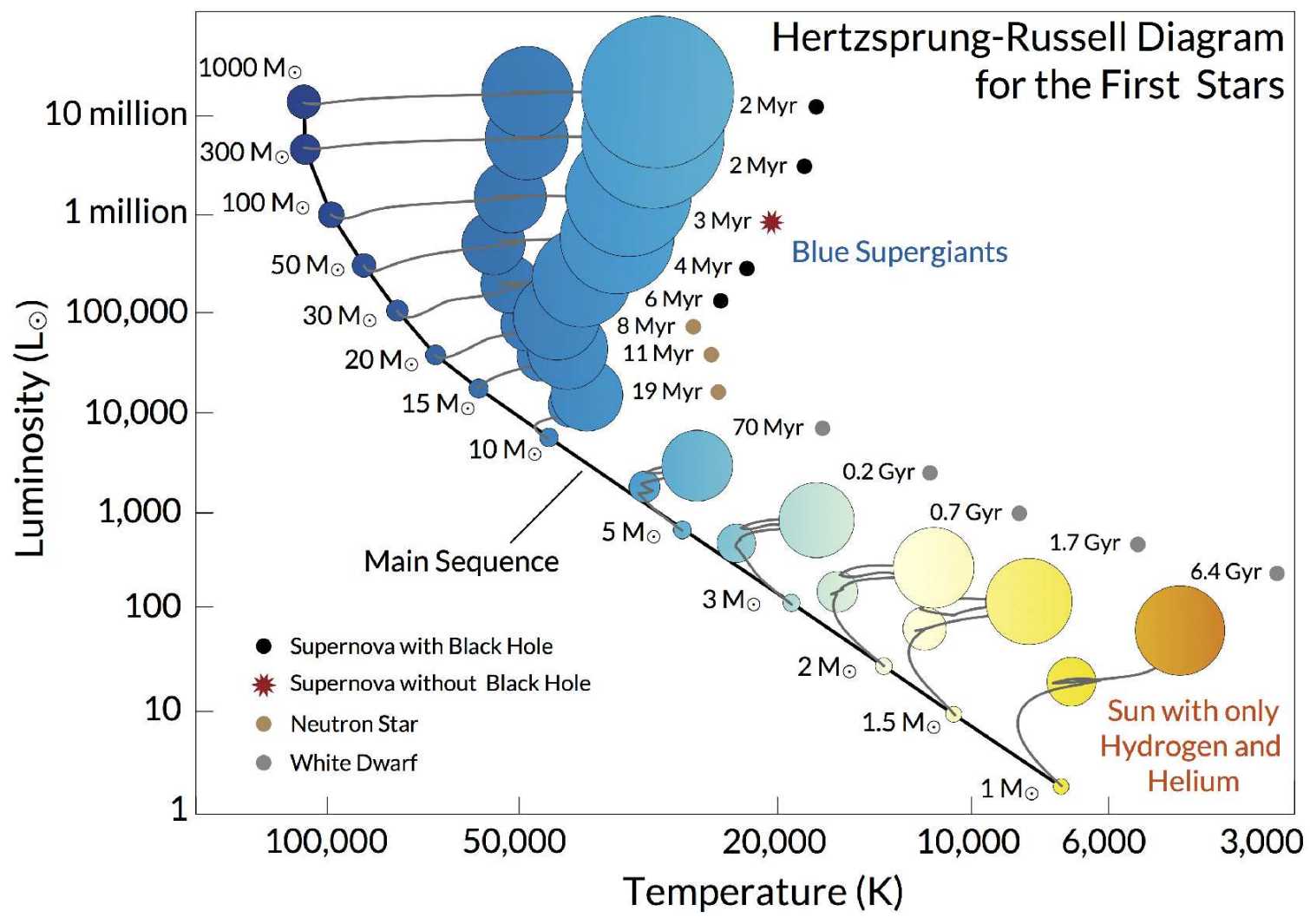
$\text{Energy(dust)} \simeq 52\% \text{ &}$
 $\text{energy(cosmic SF)} \simeq 48\%$
of EBL \Rightarrow dust wins!

Diffuse $1-4\mu\text{m}$ sky $\lesssim 0.1 \text{ nW/m}^2/\text{sr}$
or $\text{SB(K)} \gtrsim 31 \text{ mag/arcsec}^2$:

- 1) possibly from Pop III stars at $z \simeq 7-17$, and/or
- 2) their stellar-mass BH accretion disks ($z \simeq 7-8$).

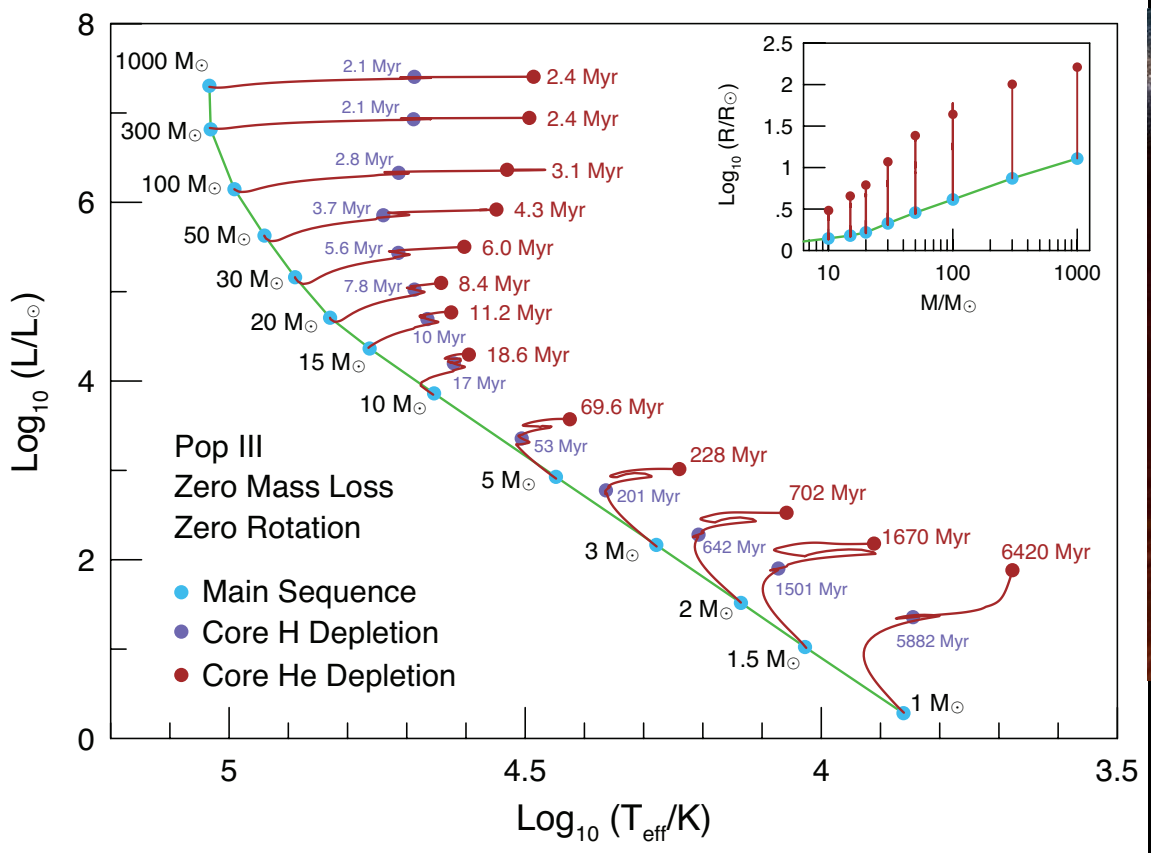
This can make Pop III stars or their BH accretion disks visible to JWST at $\text{AB} \lesssim 28-29$ mag.

- Requires using the best lensing clusters and monitoring caustic transits.
- JWST must monitor best lensing clusters throughout its lifetime.



First Stars (“Pop III”) HR-diagram: MESA stellar evolution models for zero metallicity (Windhorst, Timmes, Wyithe et al. 2018, ApJS, 234, 41):

- 30–1000 M_{\odot} Pop III ZAMS stars live $\sim 10 \times$ shorter than 2–5 M_{\odot} Pop III stars in their Giant Branch stage.
- Hence, 2–5 M_{\odot} AGB companion stars can feed the LIGO-mass BHs left over from $M \gtrsim 30 M_{\odot}$ Pop III stars (assuming binaries in 2nd generation).

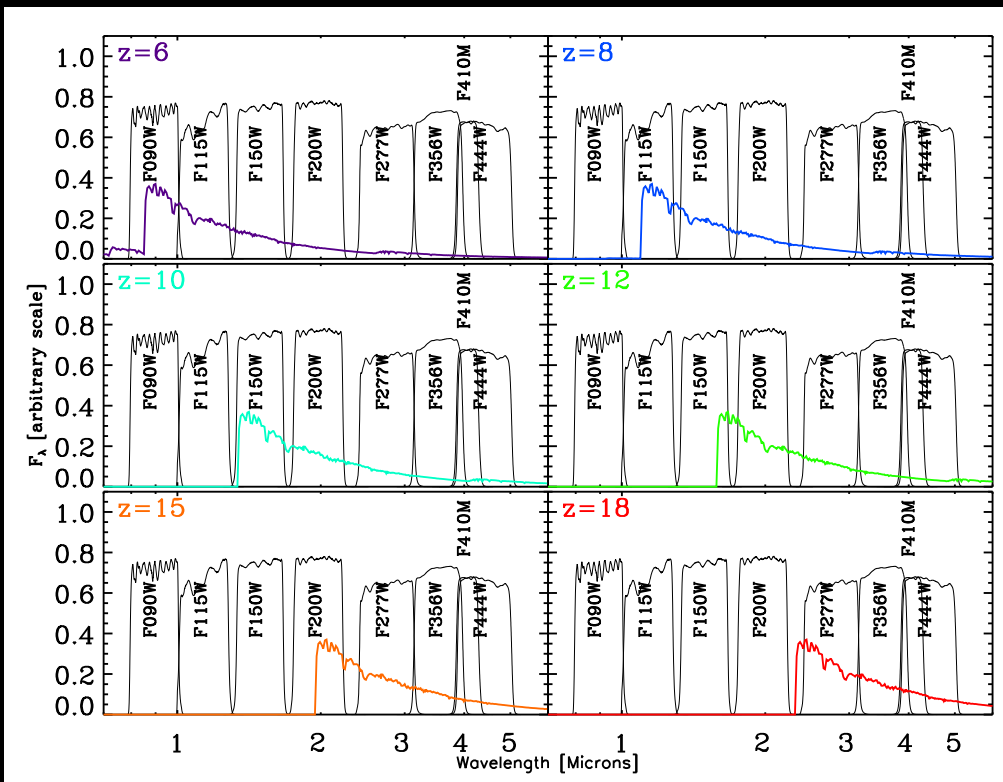
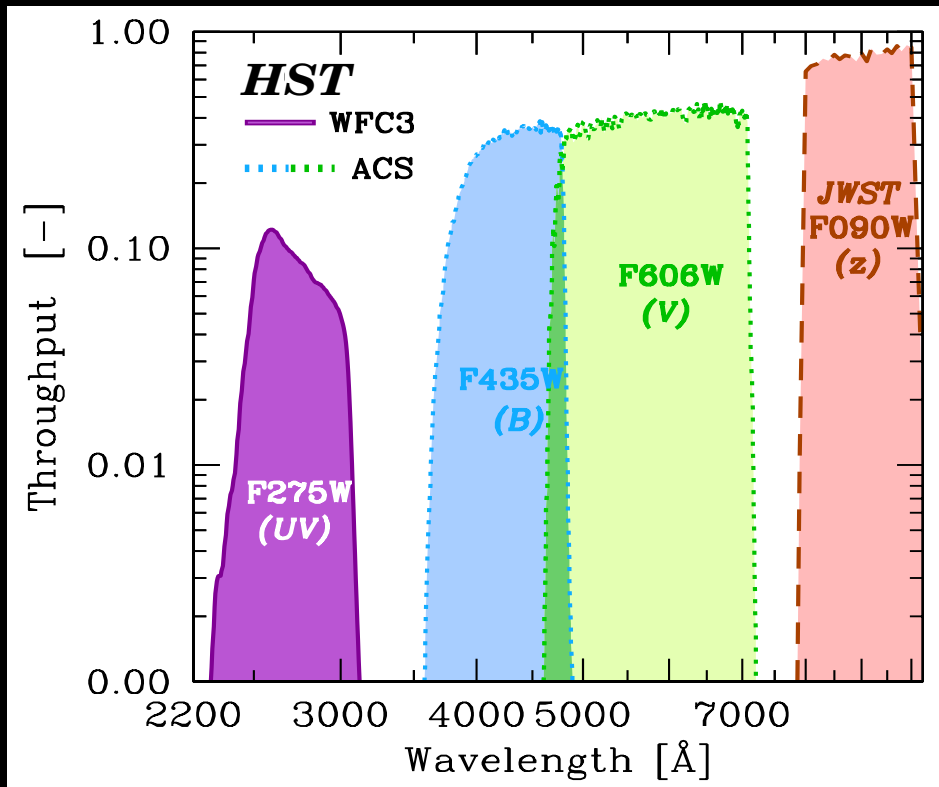


- Multicolor accretion-disk models for stellar-mass black holes [RIGHT]: For $M_{BH} \simeq 5\text{--}700 M_{\odot}$, accretion disks radii and luminosities are similar to those of Pop III AGB stars, when the BH is fed by a Roche lobe-filling lower-mass companion star on the AGB (which live $\gtrsim 10\times$ longer).
- Assumes 2nd generation O-stars have high enough Fe/H ($\gtrsim 10^{-4} Z_{\odot}$) that 2–5 M_{\odot} AGB companion stars exist and feed these LIGO-mass BHs.
- This may make stellar-mass black hole accretion disks at $z \gtrsim 7$ at least as likely to be seen via caustic transits as the Pop III stars themselves.

(3) Conclusions for Pop III Star/BH Accretion Disk caustic transits

- If $M \gtrsim 30 M_{\odot}$ Pop III ZAMS stars ($AB \sim 37-42$ mag at $z \gtrsim 7$) have $\mu \gtrsim 10^4-10^5$ during caustic transits, they could be detectable for a few months to $AB \lesssim 29$ mag with JWST. Rise times of a few hours.
- Pop III stellar mass black hole ($M \gtrsim 20 M_{\odot}$) accretion disks could be similarly detectable, *and* live $\sim 10 \times$ longer than their ZAMS stars.
- JWST can detect individual Pop III objects at $AB \lesssim 28-29$ mag via cluster caustic transits if magnifications $\mu \simeq 10^4-10^5$ (*i.e.*, ICL microlensing doesn't dominate cluster caustics).
- In the case of significant micro-lensing by ICL objects, 30 m telescopes + MCAO can follow this up for decades, but only at $\lambda \simeq$ at 1–2 μm .
- Expect $\lesssim 1$ caustic transit/yr at $z \gtrsim 7$ when JWST monitors $\gtrsim 3$ clusters.
- Stellar-mass BH accretion disks may dominate caustic transits at $z \gtrsim 7$.
- JWST GO community should anticipate this, and plan for it.

SPARE CHARTS

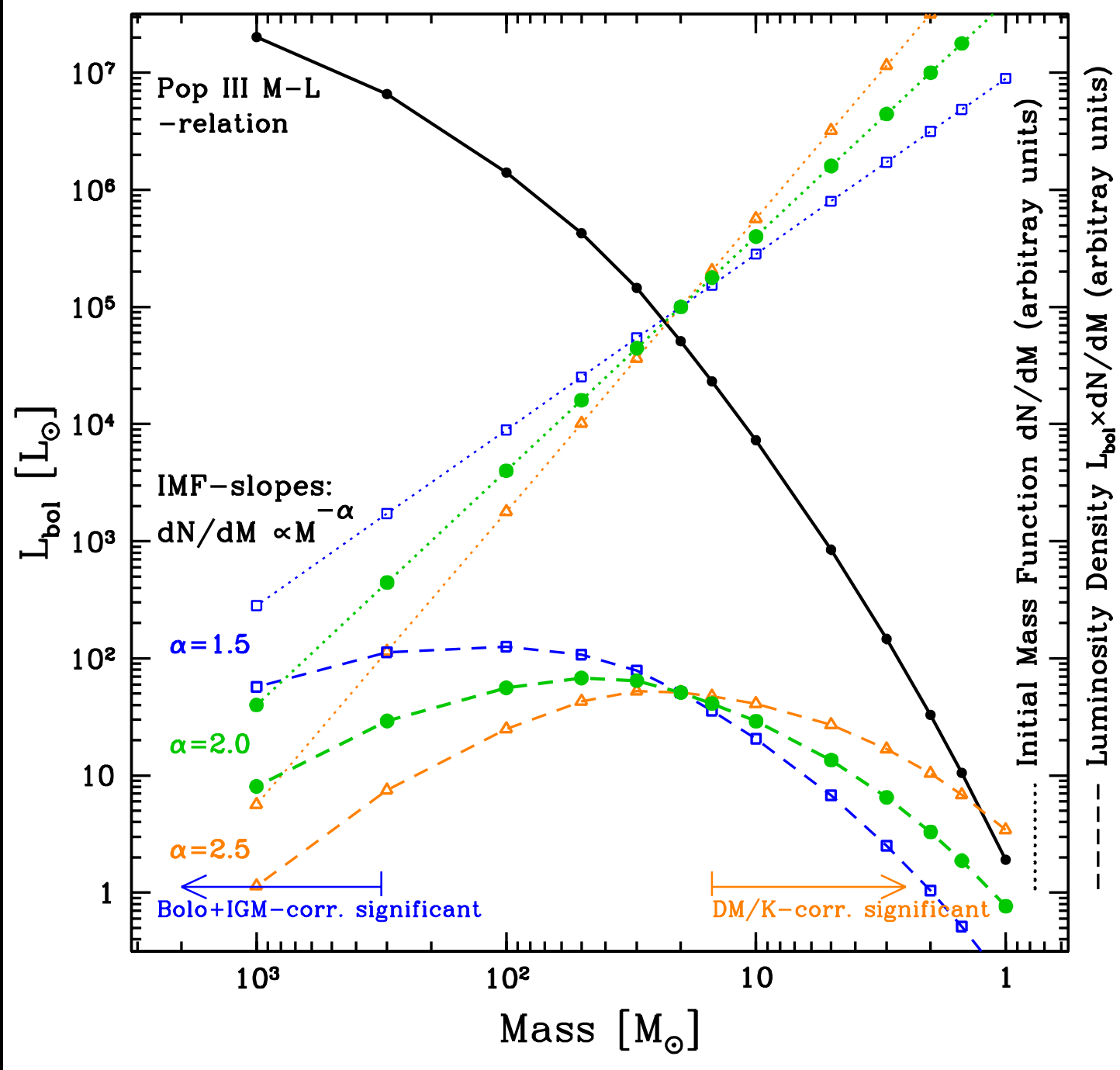


[LEFT] HST UV-vis filters complement the JWST NEP community field:

- HST adds λ 's inaccessible to JWST, or where HST has better PSF.

[RIGHT] Standard 8-band $0.8\text{--}5 \mu\text{m}$ filter set for JWST NIRCam.

- These are what GTO's will use as standard NIRCam filters.



Mass–Luminosity relation for zero metallicity Pop III MESA models:

For a range of IMF slopes, most Pop III star sky-SB comes from $20\text{--}300 M_{\odot}$.

Table 1. Adopted Pop III Star Physical Parameters from MESA models^a

Mass (M_{\odot})	Age (Myr)	T_{eff} (K)	log R (R_{\odot})		T_{eff} (K)		log R (R_{\odot})		Age Myr	T_{eff} (K)		log R (R_{\odot})		Age Myr	Time ^b (Myr)
			— at ZAMS —		— at Hydrogen-depletion —		— at Helium-depletion —			— at Helium-depletion —		— at Helium-depletion —			
1.0	9.28	7.266e3	-0.0581	0.2825	6.999e3	0.5119	1.3576	5882	— ^c	—	—	—	6420	538	
1.5	6.11	1.065e4	-0.0203	1.0227	1.181e4	0.3292	1.9015	1501	8.149e3	0.7913	2.1804	1670	169		
2.0	3.02	1.367e4	0.0108	1.5177	1.611e4	0.2498	2.2815	642	1.145e4	0.6685	2.5249	702	60		
3.0	1.38	1.899e4	0.0487	2.1654	2.311e4	0.1843	2.7770	201	1.736e4	0.5510	3.0138	228	27		
5.0	0.56	2.805e4	0.0911	2.9274	3.206e4	0.1903	3.3581	53	2.658e4	0.4608	3.5732	70	17		
10	0.23	4.508e4	0.1462	3.8618	4.174e4	0.3807	4.1972	17	3.938e4	0.4811	4.2968	19	1.6		
15	0.13	5.789e4	0.1803	4.3647	4.624e4	0.5401	4.6937	10	4.215e4	0.6581	4.7691	11	0.8		
20	0.09	6.754e4	0.2183	4.7082	4.864e4	0.6612	5.0240	7.8	4.386e4	0.7879	5.0975	8.4	0.6		
30	0.05	7.737e4	0.3270	5.1619	5.180e4	0.8120	5.4347	5.6	4.006e4	1.0688	5.5016	6.0	0.5		
50	0.03	8.713e4	0.4570	5.6283	5.490e4	0.9722	5.8562	3.7	3.536e4	1.3862	5.9200	4.3	0.5		
100	0.02	9.796e4	0.6147	6.1470	5.173e4	1.2610	6.3303	2.8	3.392e4	1.6437	6.3627	3.1	0.3		
300	0.02	1.074e5	0.8697	6.8172	4.882e4	1.6111	6.9301	2.1	3.165e4	2.0041	6.9631	2.4	0.3		
1000	0.02	1.080e5	1.1090	7.3047	4.807e4	1.8740	7.4288	2.1	3.122e4	2.2119	7.3549	2.4	0.3		

Windhorst, Timmes, Wyithe et al. (2018, ApJS, 234, 41):

- 30–1000 M_{\odot} Pop III stars ($Z=0.0$ Z_{\odot}) live $\sim 10 \times$ shorter than 2–5 M_{\odot} Pop III stars in their AGB stage.
- Hence, 2–5 M_{\odot} AGB companion stars can feed the LIGO-mass BHs left over from $M \gtrsim 30 M_{\odot}$ Pop III stars (assuming binaries in 2nd generation).

Table 2. Implied ZAMS Pop III Star Observational Parameters Relevant to Caustic Transit Calculations

Mass ^a	T_{eff}^b	Radius ^c	L_{bol}^d	M_{bol}^e	Bolo+IGM+K-corr ^f			ZAMS m _{UV} ^g			t_{rise}^h	transit ⁱ
ZAMS (M_{\odot})	— at ZAMS —	—	—	—	z=7	z=12	z=17	z=7	z=12	z=17	caust	rate
	(K)	(R_{\odot})	(L_{\odot})	(AB)	(AB-mag)			(AB-mag)			(hr)	(/cl/yr)
1.0	7.266e3	0.87	1.92	+4.03	+4.44	+3.13	+2.61	57.71	57.74	58.07	0.17	8×10^5
1.5	1.065e4	0.95	10.5	+2.18	+1.45	+0.42	-0.06	52.87	53.18	53.55	0.18	1.1×10^4
2.0	1.367e4	1.03	32.9	+0.95	+0.30	-0.59	-1.06	50.49	50.93	51.31	0.20	1.5×10^3
3.0	1.899e4	1.12	146.	-0.67	-0.51	-1.26	-1.72	48.06	48.64	49.03	0.22	182.
5.0	2.805e4	1.23	846.	-2.58	-0.70	-1.35	-1.80	45.96	46.65	47.04	0.24	29.1
10	4.508e4	1.40	7.28e3	-4.91	-0.22	-0.79	-1.23	44.10	44.88	45.27	0.27	5.70
15	5.789e4	1.51	2.32e4	-6.17	+0.23	-0.30	-0.75	43.30	44.10	44.50	0.29	2.78
20	6.754e4	1.65	5.11e4	-7.03	+0.56	+0.04	-0.40	42.77	43.59	43.99	0.32	1.74
30	7.737e4	2.12	1.45e5	-8.16	+0.88	+0.36	-0.08	41.95	42.78	43.17	0.41?	0.82?
50	8.713e4	2.86	4.25e5	-9.33	+1.17	+0.66	+0.22	41.08	41.91	42.31	0.55*	0.37*
100	9.796e4	4.12	1.40e6	-10.63	+1.47	+0.96	+0.52	40.08	40.91	41.31	0.80*	0.15*
300	1.074e5	7.41	6.56e6	-12.30	+1.71	+1.21	+0.77	38.64	39.48	39.88	1.43*	0.039*
1000	1.080e5	12.9	2.02e7	-13.52	+1.72	+1.22	+0.78	37.44	38.28	38.68	2.48*	0.013*

- If $M \gtrsim 30 M_{\odot}$ Pop III ZAMS stars have $\mu \gtrsim 10^4 - 10^5$ during caustic transits, they could be detectable for months to AB $\lesssim 29$ mag with JWST.
- Expect $\lesssim 1$ caustic transit/yr at $z \gtrsim 7$ when JWST monitors $\gtrsim 3$ clusters.

Table 3. Implied Red Giant Branch Pop III Star Observational Parameters Relevant to Caustic Transit Calculations

Mass ^a GB (M_{\odot})	T_{eff}^b — at Hydrogen-depletion (K)	Radius ^c (R_{\odot})	L_{bol}^d (L_{\odot})	M_{bol}^e (AB)	Bolo+IGM+K-corr ^f z=7 z=12 z=17 (AB-mag)			Giant Branch muv ^g z=7 z=12 z=17 (AB-mag)			t_{rise}^h caust (hr)	transit ⁱ rate (/cl/yr)
1.0	6.999e3	3.25	22.8	+1.35	+4.83	+3.48	+2.96	55.42	55.41	55.73	0.63	9×10^4
1.5	1.181e4	2.13	79.7	-0.01	+0.91	-0.06	-0.53	50.13	50.51	50.88	0.41	1.0×10^3
2.0	1.611e4	1.78	191.	-0.96	-0.19	-1.01	-1.47	48.08	48.60	48.99	0.34	175.
3.0	2.311e4	1.53	598.	-2.20	-0.69	-1.39	-1.84	46.35	46.99	47.38	0.30	39.8
5.0	3.206e4	1.55	2.28e3	-3.66	-0.63	-1.25	-1.70	44.95	45.67	46.07	0.30	11.8
10	4.174e4	2.40	1.57e4	-5.75	-0.34	-0.92	-1.36	43.15	43.91	44.31	0.46	2.33
15	4.624e4	3.47	4.94e4	-6.99	-0.18	-0.74	-1.19	42.06	42.84	43.24	0.67?	0.87?
20	4.864e4	4.58	1.06e5	-7.82	-0.10	-0.65	-1.09	41.32	42.11	42.51	0.88*	0.44*
30	5.180e4	6.49	2.72e5	-8.85	+0.02	-0.53	-0.97	40.41	41.20	41.60	1.25*	0.19*
50	5.490e4	9.38	7.18e5	-9.90	+0.13	-0.42	-0.86	39.47	40.26	40.66	1.81*	0.081*
100	5.173e4	18.2	2.14e6	-11.09	+0.02	-0.53	-0.98	38.17	38.96	39.36	3.52*	0.024*
300	4.882e4	40.8	8.51e6	-12.59	-0.09	-0.65	-1.09	36.57	37.35	37.75	7.88*	0.006*
1000	4.807e4	74.8	2.68e7	-13.83	-0.12	-0.67	-1.12	35.29	36.07	36.47	14.44*	0.002*

- If $M \gtrsim 20 M_{\odot}$ Pop III RGB stars have $\mu \gtrsim 10^4$ – 10^5 during caustic transits, they could be detectable for a few months to AB $\lesssim 29$ mag with JWST.
- Note the combined Bolometric+IGM+K-corrections are more advantageous for Pop III RGB stars.

Table 4. Implied AGB Pop III Star Observational Parameters Relevant to Caustic Transit Calculations

Mass ^a	T_{eff}^b	Radius ^c	L_{bol}^d	M_{bol}^e	Bolo+IGM+K-corr ^f	AGB m _{UV} ^g			t_{rise}^h	transit ⁱ		
AGB	— at Helium-depletion —				z=7	z=12	z=17	z=7	z=12	z=17	caust	rate
(M_{\odot})	(K)	(R_{\odot})	(L_{\odot})	(AB)	(AB-mag)			(AB-mag)			(hr)	(/cl/yr)
1.0	6.312e3 ^j	5.23 ^j	39.8 ^j	+0.74	+6.01	+4.57	+4.03	55.99	55.89	56.19	1.01	1.4×10^5
1.5	8.149e3	6.18	151.	-0.71	+3.36	+2.14	+1.64	51.89	52.01	52.35	1.19	4.0×10^3
2.0	1.145e4	4.66	335.	-1.57	+1.06	+0.07	-0.40	48.73	49.08	49.45	0.90	273.
3.0	1.736e4	3.56	1.03e3	-2.79	-0.36	-1.15	-1.60	46.09	46.64	47.03	0.69	28.9
5.0	2.658e4	2.89	3.74e3	-4.19	-0.72	-1.38	-1.82	44.33	45.01	45.41	0.56	6.43
10	3.938e4	3.03	1.98e4	-6.00	-0.42	-1.00	-1.45	42.82	43.57	43.97	0.58	1.71
15	4.215e4	4.55	5.88e4	-7.18	-0.33	-0.90	-1.34	41.73	42.50	42.89	0.88?	0.64?
20	4.386e4	6.14	1.25e5	-8.00	-0.27	-0.84	-1.28	40.97	41.74	42.14	1.19*	0.32*
30	4.006e4	11.7	3.17e5	-9.01	-0.40	-0.98	-1.42	39.83	40.59	40.98	2.26*	0.11*
50	3.536e4	24.3	8.32e5	-10.06	-0.55	-1.15	-1.59	38.63	39.37	39.77	4.70*	0.036*
100	3.392e4	44.0	2.31e6	-11.17	-0.59	-1.19	-1.64	37.49	38.22	38.61	8.50*	0.012*
300	3.165e4	101.	9.19e6	-12.67	-0.64	-1.26	-1.71	35.93	36.65	37.04	19.49*	0.003*
1000	3.122e4	163.	2.26e7	-13.65	-0.65	-1.28	-1.72	34.94	35.66	36.05	31.45*	0.001*

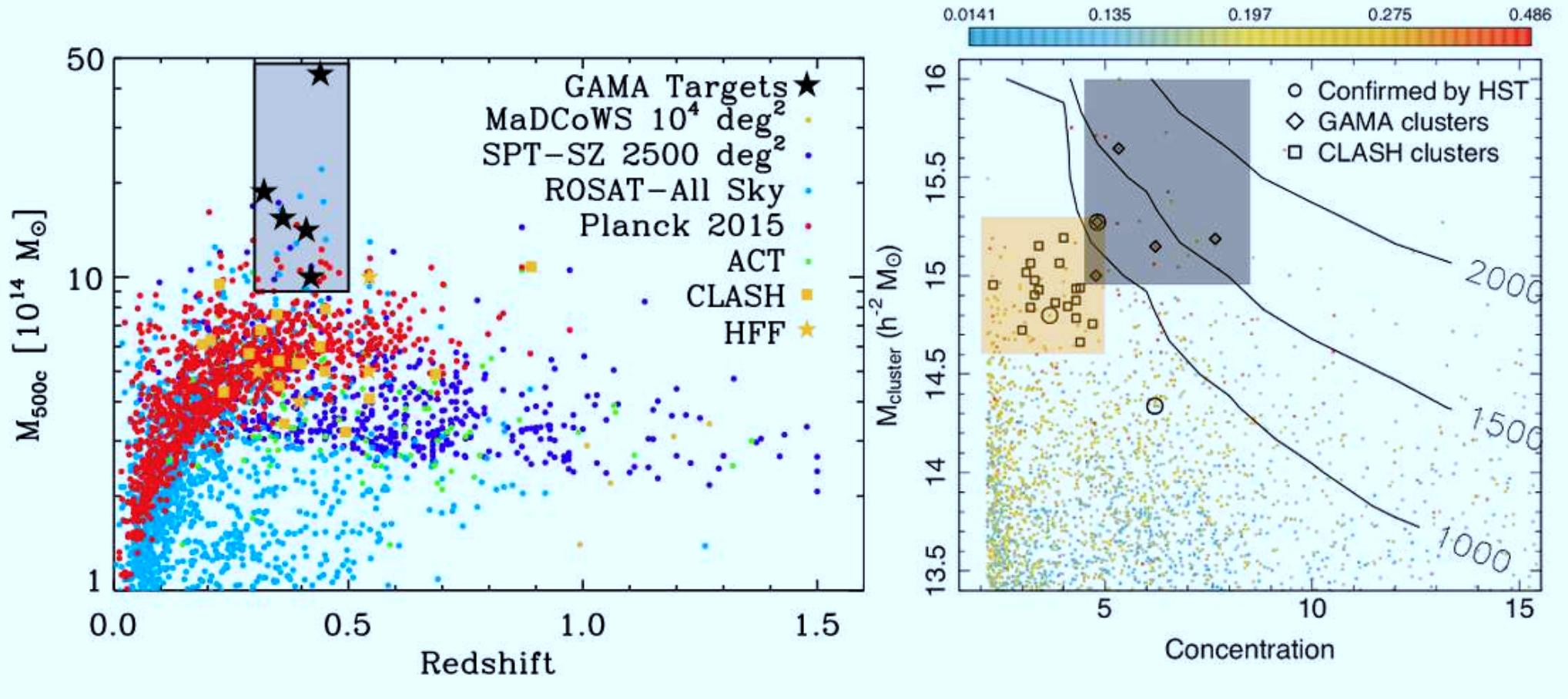
- If $M \gtrsim 20 M_{\odot}$ Pop III AGB stars have $\mu \gtrsim 10^4 - 10^5$ during caustic transits, they could be detectable for a few months to AB $\lesssim 29$ mag with JWST.
- Note the combined Bolometric+IGM+K-corrections are far more advantageous for Pop III AGB stars (especially at $z \gtrsim 12$)!

Table 5. Pop III Stellar Mass Black Hole Accretion Disk Parameters Adopted for Caustic Transit Calculations

Mass ^a	M _{compact} ^b	R _s ^c	Radius ^d	L _{bol} ^e	M _{bol} ^f	bolo+IGM+K-corr ^g	m _{AB} -limits at ^h	t _{rise} ⁱ	Transit ^j		
ZAMS		BH	— of the UV accretion disk —	z=7	z=12	z=17	z=7	z=12	z=17	(z=12)	rate
(M _⊙)	(M _⊙)	(km)	(R _⊙)	(L _⊙)	AB-mag	(AB-mag)	(AB-mag)	(AB-mag)	(hr)	(hr)	(/cl/yr)
BH accretion-disk bolometric luminosities and UV half-light radii scaling from microlensed quasars (Blackburne et al. 2011)											
30	~5.0 BH	15	1.4	$\lesssim 4.2 \times 10^4$	$\gtrsim -6.8$	-0.6	-1.4	-1.7	$\gtrsim 41.8$	$\gtrsim 42.4$	$\gtrsim 42.9$
50	~24 BH	72	3.0	$\lesssim 2.0 \times 10^5$	$\gtrsim -8.5$	-0.4	-1.2	-1.5	$\gtrsim 40.3$	$\gtrsim 40.9$	$\gtrsim 41.4$
100	~65 BH	195	4.9	$\lesssim 5.4 \times 10^5$	$\gtrsim -9.6$	-0.2	-0.9	-1.3	$\gtrsim 39.4$	$\gtrsim 40.0$	$\gtrsim 40.5$
300	~230 BH	690	9.2	$\lesssim 1.9 \times 10^6$	$\gtrsim -11.0$	-0.2	-1.0	-1.3	$\gtrsim 38.1$	$\gtrsim 38.6$	$\gtrsim 39.2$
1000	~720 BH	2160	16.3	$\lesssim 6.0 \times 10^6$	$\gtrsim -12.2$	-0.2	-0.9	-1.3	$\gtrsim 36.8$	$\gtrsim 37.5$	$\gtrsim 37.9$
BH accretion-disk bolometric luminosities and UV half-light radii estimated from multi-color thin-disk model											
30	~5.0 BH	15	1.9	$\lesssim 3.1 \times 10^4$	$\gtrsim -6.5$	-0.6	-1.4	-1.7	$\gtrsim 42.1$	$\gtrsim 42.8$	$\gtrsim 43.2$
50	~24 BH	72	4.5	$\lesssim 1.8 \times 10^5$	$\gtrsim -8.4$	-0.4	-1.2	-1.5	$\gtrsim 40.4$	$\gtrsim 41.1$	$\gtrsim 41.5$
100	~65 BH	195	7.8	$\lesssim 5.9 \times 10^5$	$\gtrsim -9.7$	-0.2	-0.9	-1.3	$\gtrsim 39.3$	$\gtrsim 40.0$	$\gtrsim 40.4$
300	~230 BH	690	15.8	$\lesssim 2.0 \times 10^6$	$\gtrsim -11.0$	-0.2	-1.0	-1.3	$\gtrsim 38.0$	$\gtrsim 38.6$	$\gtrsim 39.1$
1000	~720 BH	2160	29.8	$\lesssim 6.6 \times 10^6$	$\gtrsim -12.3$	-0.2	-0.9	-1.3	$\gtrsim 36.7$	$\gtrsim 37.4$	$\gtrsim 37.8$

- If $M \gtrsim 20 M_{\odot}$ Pop III stellar mass black hole accretion disks have $\mu \gtrsim 10^4$ – 10^5 during caustic transits, they could be detectable for a few months to AB $\lesssim 29$ mag with JWST. Rise times \sim hours–1 day; Decay times $\lesssim 0.4$ yr.
- Note the combined Bolometric+IGM+K-corrections are also more advantageous for Pop III stellar-mass black hole accretion disks.

Multi- λ model: $T \propto r^{-3/4}$; $T_{max} \simeq 10 \left(\frac{M_{BH}}{100} \right)^{-3/8}$ keV; $r_{hl} \propto M_{BH}^{1/2}$.



What are the best lensing clusters for JWST to see First Light objects?:

[LEFT] Best lensing clusters vs. ROSAT, Planck, SPT, MaDCoWS.

[RIGHT] Best lensing clusters compared to CLASH clusters.

(Contours: Number of lensed JWST sources at $z \approx 1-15$ to $\text{AB} \lesssim 31$ mag).

- Resulting sweet spot for JWST lensing of First Light Objects ($z \gtrsim 10$):

Redshift: $0.3 \lesssim z \lesssim 0.5$; Mass: $10^{15-15.6} M_\odot$; Concentration: $4.5 \lesssim C \lesssim 8.5$

(4) What are the best lensing clusters to monitor caustic transits?

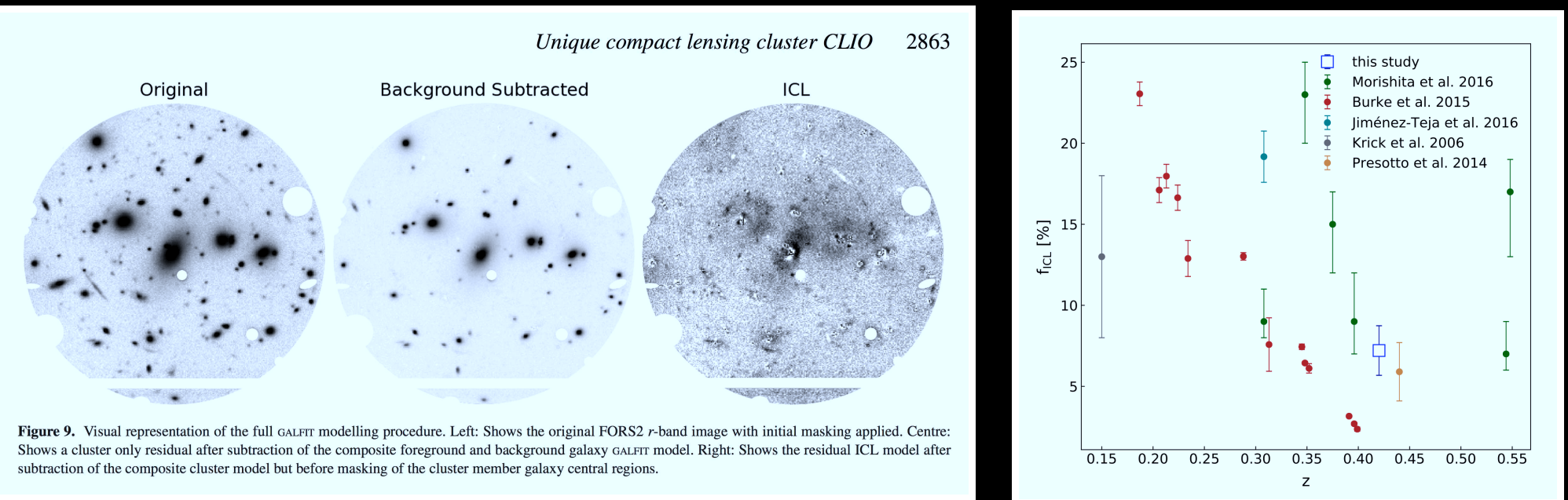


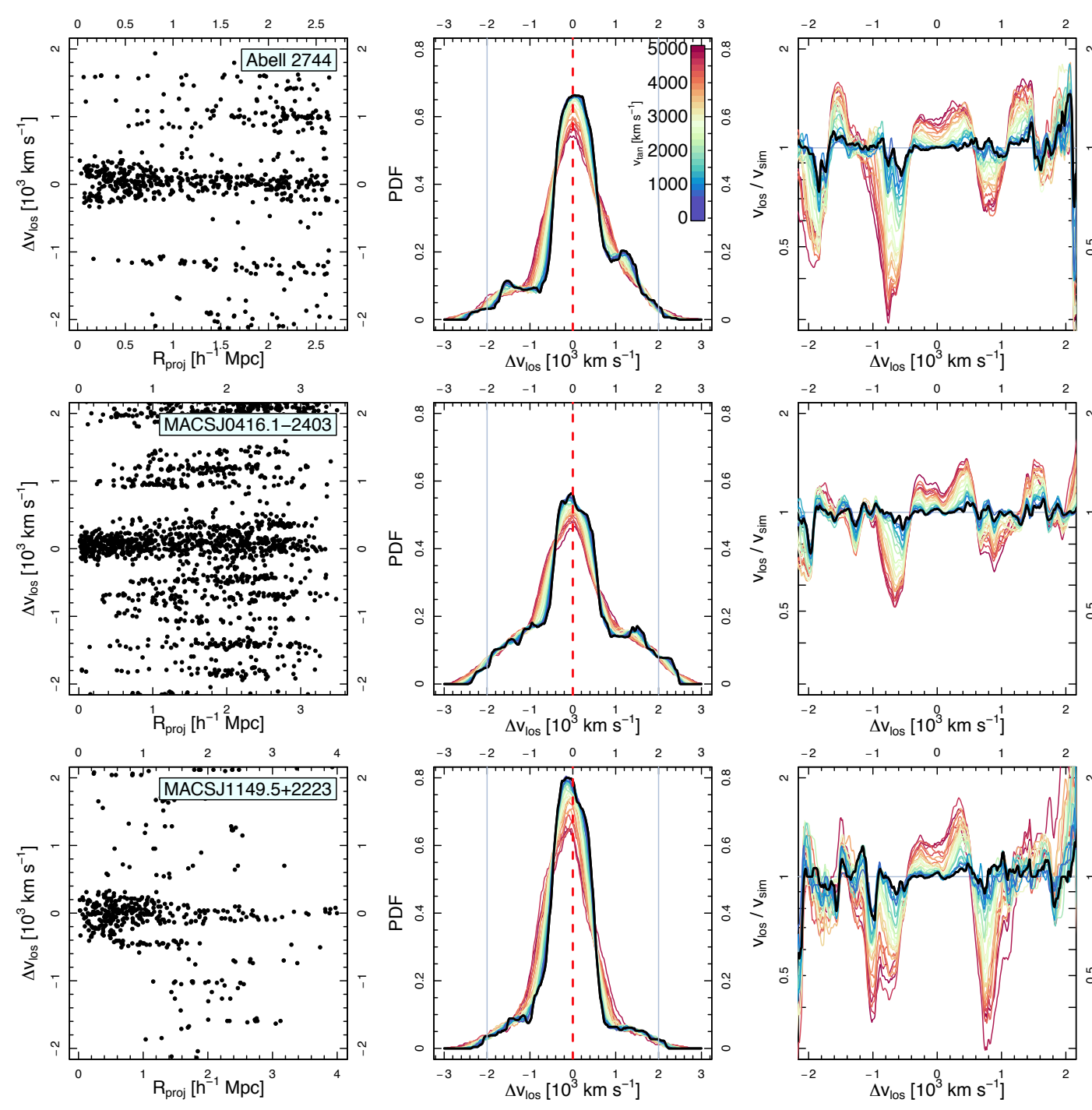
Figure 9. Visual representation of the full GALFIT modelling procedure. Left: Shows the original FORS2 *r*-band image with initial masking applied. Centre: Shows a cluster only residual after subtraction of the composite foreground and background galaxy GALFIT model. Right: Shows the residual ICL model after subtraction of the composite cluster model but before masking of the cluster member galaxy central regions.

Griffiths et al. (2018 MNRAS, 475, 2853): GAMA cluster at $z \approx 0.42$ found through mass-concentration selection. Has 89 VLT MUSE members:

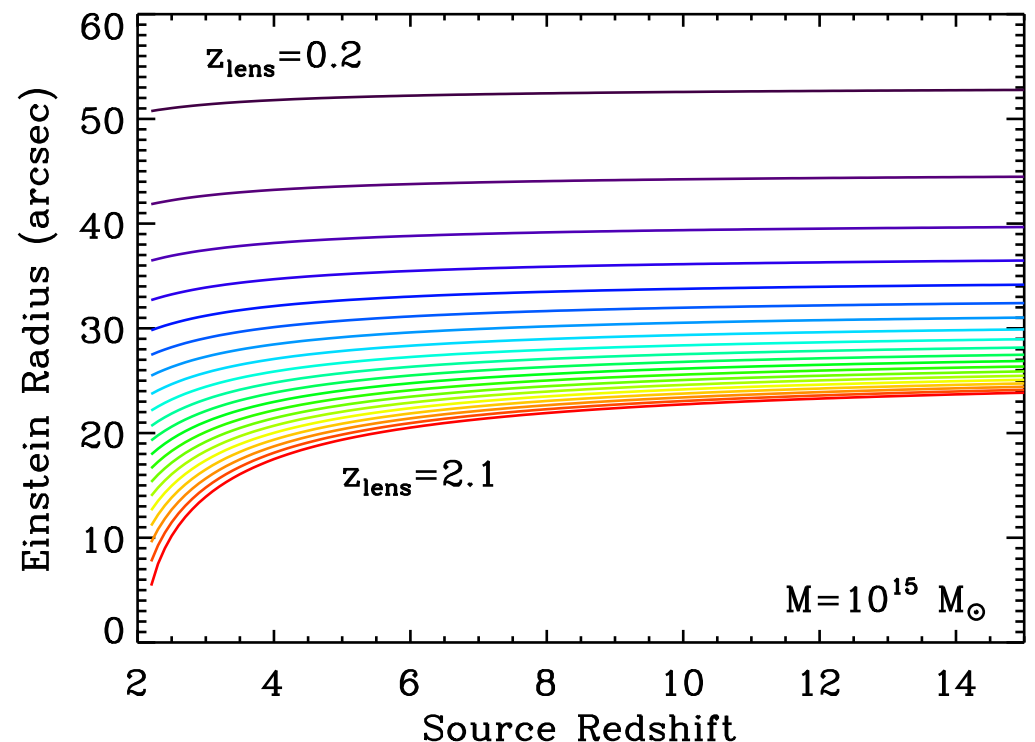
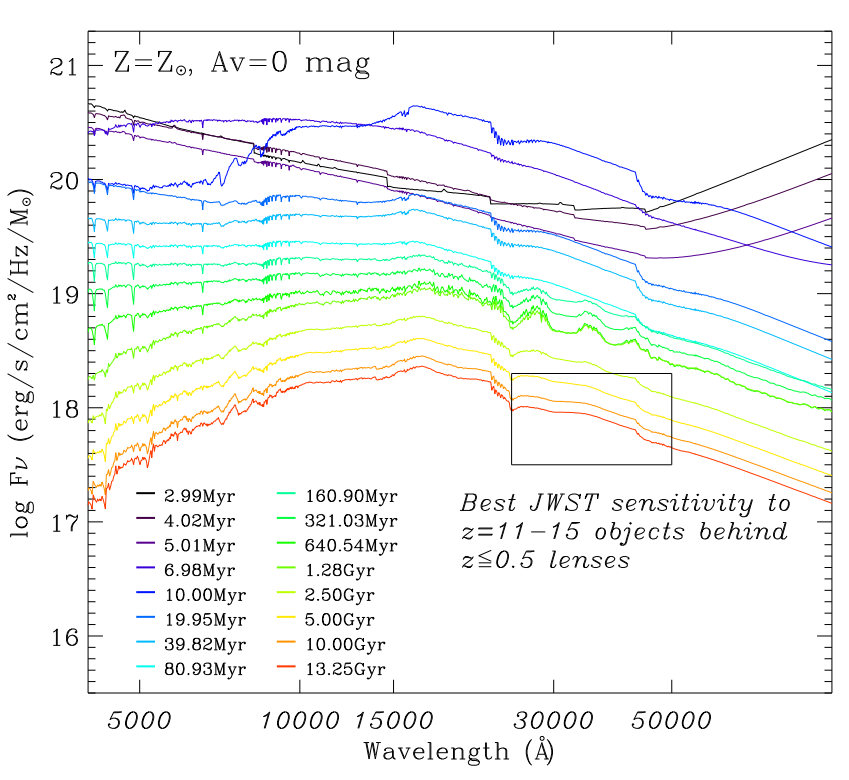
- Cluster has minimal ICL near the critical curves, optimal for caustic transit studies. Can see several arcs clearly in ground-based images.
- JWST should monitor clusters with minimal ICL near the critical curves to minimize microlensing and maximize caustic transit magnifications.

Trumpet diagrams for JWST lensing clusters from ground-based spectroscopic $N(z)$ (Windhorst⁺ 2018):

- 1) Add random space velocity v_{sp} to clusters.
- 2) Projected v_T must be $\lesssim 1000 \text{ km/s}$ for v_{sp} not to unduly disturb radial $N(z)$.
- 3) Best clusters (Bullet) for caustic transits can have $v_T \lesssim 2700 \text{ km s}^{-1}$.



- JWST should monitor such clusters during its lifetime for caustic transits.



Galaxy SEDs for different ages: peak at $\lambda_{rest} \approx 1.6 \mu\text{m}$ (Kim et al. 2017).

JWST-NIRCam peaks in sensitivity for $\lambda = 3-5 \mu\text{m}$, where Zodi is lowest.

Sweet spot for lensing cluster $z \lesssim 0.5$: Zodi-gain mitigates $(1+z)^4$ -dimming.

- Minimizes effects from near-IR K-correction and ambient ICL.
- Lower redshift clusters also have higher (virialized) masses and much larger Einstein radii.
- This is critical for optimizing caustic transit detections away from ICL.